Dynamic speckle image segmentation using self-organizing maps

2016 J. Opt. 18 085606

(http://iopscience.iop.org/2040-8986/18/8/085606)

IOP Publishing Journal of Optics
J. Opt. 18 (2016) 085606 (11pp) doi:10.1088/2040-8978/18/8/085606

Dynamic speckle image segmentation using self-organizing maps

Ana L Dai Pra[2], Gustavo J Meschino[1], Marcelo N Guzmán[1], Adriana G Scandurra[1], Mariela A González[1], Christian Weber[3,4], Marcelo Trivi[3], Héctor Rabal[3] and Lucía I Passoni[1,5]

[1] Instituto de Investigaciones Científicas y Tecnológicas en Electrónica. Laboratorio de Bioingeniería. CONICET—Universidad Nacional de Mar del Plata. Juan B. Justo 4302. Mar del Plata. Argentina
[2] Grupo de Inteligencia Artificial Aplicado a Ingeniería. Facultad de Ingeniería. Universidad Nacional de Mar del Plata. Juan B. Justo 4302. Mar del Plata. Argentina
[3] Centro de Investigaciones Ópticas (CONICET La Plata—CIC). Facultad de Ingeniería. Universidad Nacional de La Plata. Calle 1 y 47—La Plata. Argentina
[4] Facultad de Ciencias Agrarias y Forestales. Universidad Nacional de La Plata. Calle 60 y 119. La Plata. Argentina

E-mail: daipra@fi.mdp.edu.ar, gmeschin@fi.mdp.edu.ar, marcelo.guzman@fi.mdp.edu.ar, scandu@fi.mdp.edu.ar, mazulgonzalez@fi.mdp.edu.ar, cweber@ciop.unlp.edu.ar, marcelo@ciop.unlp.edu.ar, hrabal@ing.unlp.edu.ar and lpassoni@fi.mdp.edu.ar

Received 19 January 2016, revised 10 May 2016
Accepted for publication 3 June 2016
Published 1 July 2016

Abstract

The aim of this work is to build a computational model able to automatically identify, after training, dynamic speckle pattern regions with similar properties. The process is carried out using a set of descriptors applied to the intensity variations with time in every pixel of a speckle image sequence. An image obtained by projecting a self-organized map is converted into regions of similar activity that can be easily distinguished. We propose a general procedure that could be applied to numerous situations. As examples we show different situations: (a) an activity test in a simplified situation; (b) a non-biological example and (c) biological active specimens. The results obtained are encouraging; they significantly improve upon those obtained using a single descriptor and will eventually permit automatic quantitative assessment.

Keywords: dynamic speckle, optical processing, self-organizing maps, computational intelligence, SOM

(Some figures may appear in colour only in the online journal)

1. Introduction

Dynamic speckle patterns have been used to assess issues of interest in different fields, such as biology (seed analysis, animal sperm motility), medicine (capillary blood flow), industry (discovering bruising in fruits, paint drying, monitoring of ice cream melting, yeast bread, gels), among others. An extensive list of descriptors, which provide numerical measurement that characterize the activity of the specks, has been presented in the literature. Most of them achieve good performance to detect, in some specific way, the dynamic characteristics of the sample phenomenon (Rabal and Braga 2008).

The physical description of the dynamics is usually poorly known or it is not known at all. Only a few descriptors can be related to physical counterparts. Most of the descriptors are heuristic or based on statistics, and they are chosen taking into account their ability to screen out some specific property (Dai Pra *et al* 2015). Similar to surface roughness, several measurements are required for its full characterization; intensity variation evaluation cannot be characterized by measurements of a single parameter. It is expected that the simultaneous use of a set of descriptors improves the ability to identify activity differences in regions of interest. As a

[5] Author to whom any correspondence should be addressed.

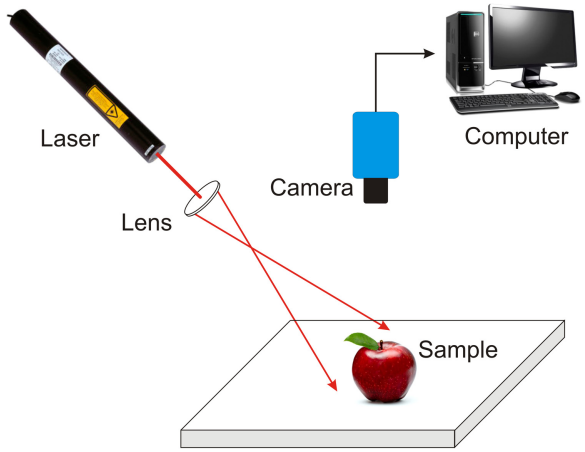

Figure 1. Generic optical setup for laser speckle image acquisition.

consequence, a set of descriptors is expected to present better performance than a single one for every experimental situation. Two ways (at least) can be used to choose and combine this set of descriptors outputs.

Supervised learning seems an adequate way when a particular known target is sought. Then, identified samples with known characteristic descriptors sets are used to identify in unknown samples the presence of regions with similar behaviour to those used for learning (Passoni *et al* 2013a).

In the other way, when the target is to search for homogeneity of the sample, the presence of unknown phenomena, or the presence of different phases, it is better to be guided by the phenomenon itself. Then, unsupervised learning can be expected to distinguish between regions of different dynamics provided appropriate descriptors are considered. The right descriptors for unpredicted, unknown phenomena cannot be determined *a priori*.

The usual undefined term 'activity level' seems inappropriate when simultaneous several descriptors with different meanings are considered. Perhaps, the term 'activity similarity' could be used instead, reflecting that the classification output refers to similar dynamics as seen from the descriptor outputs.

It is desirable to find a method of detecting biospeckle dynamics and to distinguish between sample components that would be dictated by the phenomenon itself, and diverse regions in a sample that are not known to be present *a priori*.

The aim of this work is to build models able to automatically characterize dynamic speckle patterns in order to identify regions with similar properties. To address this task we propose to apply computational intelligence (CI) hybrid techniques (Engelbrecht 2007).

Recently, we proposed using a supervised learning procedure for a dynamic speckle image based on the application of a naïve Bayes statistical classifier comprising the use of several descriptors (Passoni *et al* 2013a). In that work, speckle patterns were analysed by training a supervised neural network by making it learn certain features based on already known descriptors with the help of a (human) supervisor. After the learning procedure the neural network was able to recognize regions in unknown samples that were similar to the learned ones.

In this new work, which can be considered a natural continuation of the former, supervised training is not required as the proposed algorithm itself looks for regions with similar features. It constitutes a substantial improvement over the procedure mentioned above as overlooked regions by the human supervisor are evaluated on an objective basis. Known descriptors from the literature are considered.

We propose a method for performing the visualization of sample regions using image sequences of laser speckle patterns coming from different situations: a) activity test in a simplified situation using a paint drying experiment, b) inhomogeneous illuminated surface of a wet painted sample, and c) an active biologic specimen (fruit). Previously, bacteria (Guzmán *et al* 2010) and seeds (Passoni *et al* 2013b) were also tested and preliminary results were presented.

Image sequences are used as input to an unsupervised neural network, such as a self-organizing map (SOM) (Kohonen 2001). This type of neural network has also been used to characterize a chemotaxis assay and regions were neatly differentiated according to the bacterial motility within the sample (Meschino *et al* 2010). SOMs have also been proposed as a clustering method in those cases where the sensitivity of the activity measurement of dynamic speckle images needs to be improved (Etchepareborda *et al* 2010).

A multi descriptor approach driven by the dynamics of the phenomenon itself does not require the assistance of an expert in the learning stage and it shows better performance than those provided by single descriptor analysis.

The main contribution of this work is a technique for colouring images obtained from dynamic speckle laser videos, in order to help an automated system to identify a particular region of interest depending on the application.

2. Materials and methods

In this section, after describing the acquisition setup, the proposed processing method is detailed. Some descriptors are reviewed and the SOM is briefly explained to understand the proposed algorithm in order to obtain pseudo coloured images that allow the discovery of different regions in the speckle images.

2.1. Equipment setup, signal acquirement and feature extraction

The samples were illuminated with an expanded and attenuated 10 mW He–Ne laser. The subjective speckle images were then registered using a charge-coupled device (CCD) camera (Pulnix TM-6CN, CCIR Standard, interlaced scanning, pixel size $8.6 \times 8.3\ \mu$m, objective lens $f = 50$ mm), digitized by a frame grabber to 8 bits and stored in the memory of a personal computer. For the speckle to be well resolved, we chose the speckle size to be about four to five pixels by adjusting the diaphragm aperture $\left(\frac{f}{\#} = 16\right)$.

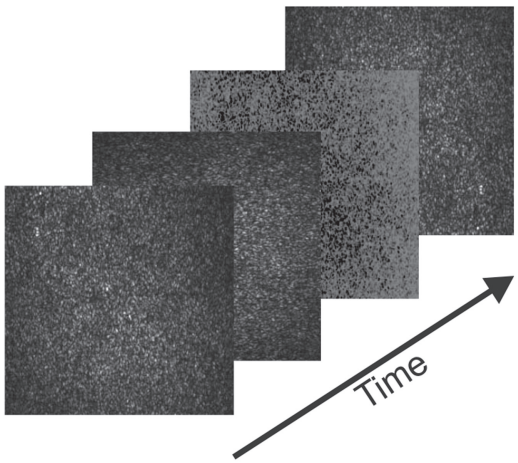

Figure 2. Laser speckle sequence of images.

Figure 1 shows the generic experimental setup for acquisition and storage of the so-called subjective images of a sample showing dynamic speckle.

The CCD objective was focused on the surface of the sample and the laser intensity was kept constant during data acquisition.

To evaluate the dynamics within stationary periods of time, image sequences were registered using a 4 Hz sampling frequency, as shown schematically in figure 2. The intensity from each image pixel was converted into a time series to be processed by feature extraction. Therefore, numerical descriptors are obtained for every pixel location.

Several descriptors have been developed, which have different performance in relation to effectiveness and computational cost (Rabal and Braga 2008). In this work, the computed descriptors belong mainly to the time domain; they are those with the lowest computational cost. However, a descriptor in the time-frequency domain was also computed. The latter presents the best ratio between performance and computational cost (Dai Pra *et al* 2015).

2.2. Feature extraction and selection

In this section, definitions for the descriptors are given, where $I_k(x, y)$ is the intensity level in the image k, $k = 1, 2, \ldots N$, for the pixel located in (x, y), and N is the number of images in the acquired sequence. All of them are time-domain descriptors (sections 2.2.1 to 2.2.6) except the last one (section 2.2.7), which corresponds to the time-frequency domain.

Given that designers are experienced in dynamic speckle pattern recognition, the feature selection process that provides the elements of the input vector to the SOM, is purely heuristic (Guyon and Elisseeff 2003). The criterion used is the selection of those descriptors that contribute to obtaining an image where the region of interest is easily segmented considering, where possible, descriptors requiring the lowest computational cost.

In this work we propose:

- subtraction average (SA) of consecutive pixel intensities,
- averaged differences (AD),
- weighted generalized differences (WGDs),
- dynamic range (DR),
- significant changes count (SCC),
- fuzzy granularity (FG),
- Shannon wavelet entropy (SWE) based descriptor.

2.2.1. SA of consecutive pixel intensities. This descriptor considers two consecutive elements of the time speckle pattern, and it is computed as:

$$SA_{(x,y)} = \sum_{k=1}^{N-1} |I_k(x, y) - I_{k+1}(x, y)|. \tag{1}$$

2.2.2. AD. This descriptor was introduced by Fujii *et al* (Fujii *et al* 1985), also known as Fujii's descriptor. The difference between contiguous samples is weighted by the local average by the following expression:

$$AD_{(x,y)} = \sum_{k=2}^{N} \frac{|I_k(x, y) - I_{k-1}(x, y)|}{|I_k(x, y) + I_{k-1}(x, y)|}. \tag{2}$$

2.2.3. WGDs. Although the AD descriptor is very suitable for many applications, it suffers from two disadvantages: it is very sensitive to noise in regions of low intensity values and it is not suitable for detecting slow varying speckle signals. In order to adapt it to these situations, a descriptor called generalized differences (GD) was proposed (Arizaga *et al* 2002), where intensity variations in different time scales are taken into account using the following expression:

$$GD_{(x,y)} = \sum_{n}\sum_{l} |I_n(x, y) - I_{n+l}(x, y)|, \tag{3}$$

where n and l are indices spanning all the possible numbers of the registered images. As every $I_n(x, y)$ value is subtracted from every other value in $I(x, y)$, the result does not depend on the sequence. This descriptor is thus very sensitive to the number of samples.

An additional weight p was later added to the GD descriptor with the aim of controlling its sensitivity. The elements of this vector allow giving different weights according to the gap of each subtraction:

$$WGD_{(x,y)} = \sum_{n=1}^{N-p}\sum_{l=1}^{p} |I_n(x, y) - I_{n+l}(x, y)|\, p_l. \tag{4}$$

This resulting descriptor was found to be useful for detecting different types of activities. However, the selection of p is empirical, restricting its application from the practical point of view.

2.2.4. DR. This is computed as the difference between the maximum and the minimum value of the intensity in each evaluated time series. The potential of this feature lies in its fast computation and its ability to discriminate regions of

coarse different activity:

$$DR_{(x,y)} = \max_{k=1,N}\{I(x,y)_k\} - \min_{k=1,N}\{I(x,y)_k\}. \quad (5)$$

2.2.5. SCC. Given a sequence of images, for each pixel this descriptor counts how many times there is a substantial change in intensity (absolute intensity difference above a threshold t), between an image and the following one in the sequence:

$$SCC_{(x,y)} = \frac{1}{(N-1)}\sum_{k=1}^{N-1}\delta_k(x,y), \quad (6)$$

where $\delta_k(x,y) = \begin{cases} 1 & \text{if } |I_{k+1}(x,y) - I_k(x,y)| \geqslant t \\ 0 & \text{if } |I_{k+1}(x,y) - I_k(x,y)| < t \end{cases}$.

The threshold t is computed based on the first two images in the sequence. Its value is the average absolute intensity difference, between both images, across all pixels (computed only on those pixels having absolute difference above zero):

$$t = \underset{(x,y)\in k}{\text{mean}}\{|I_2(x,y) - I_1(x,y)| / I_2(x,y) \neq I_1(x,y)\}. \quad (7)$$

2.2.6. FG. This descriptor quantifies the time intensity variations. The intensity series corresponding to the pixel (x, y) is transformed into a series of fuzzy granules characterized by three fuzzy sets: light, medium and dark ($i = 1, 2, 3$), corresponding to overlapped intervals of intensity values, and defining the membership of the intensity value $I_k(x,y)$ to each fuzzy set i as $\mu_i[I_k(x,y)]$:

$$FG_{(x,y)} = \sum_{n=2}^{N}\sum_{i=1}^{3}\frac{\text{suc}_i(n)}{N}, \quad (8)$$

where

$$\text{suc}_i(n) = \begin{cases} 1 & \text{if } \mu_i(I_{k-1}(x,y)) \neq 0 \text{ and } \mu_i(I_k(x,y)) = 0 \\ 0 & \text{other case} \end{cases}$$

indicates the ending of a succession of values belonging to the same fuzzy set, i.e. FG is the number of granules registered in N samples. The fuzzy set parameters of $\mu_i[I_k(x,y)]$ are obtained from the intensity histogram of a speckle pattern, tuning this characteristic to a particular sample acquisition.

2.2.7. SWE based descriptor. According to information theory, entropy is a relevant measure of order in a dynamical system. By using entropy, no specific distribution needs to be assumed. The spectral entropy as defined from the Fourier power spectrum shows a natural approach to quantifying the degree of order of a complex signal, indicating the spread level of the signal power spectrum. The stationary condition for applying the Fourier transform (FT) is not ensured in time speckle patterns. To deal with these limitations, time evolving entropy can be defined from a time-frequency representation of the signal as provided by the discrete wavelet transform (DWT). The SWE of the intensity time series at (x, y) is computed using Daubechies wavelet (order = 2) (Rosso *et al* 2001):

$$SWE_{(x,y)} = -\sum_{i=1}^{K} q_i \log(q_i), \quad (9)$$

where K denotes the total number of sub-band signals obtained from the DWT of the intensity time series and q_i is the relative wavelet energy computed as:

$$q_i = \frac{E_i}{E_t}, \quad (10)$$

where E_i denotes the energy of the ith sub-band signal computed from the wavelet coefficients. Then the total signal energy is given by:

$$E_t = \sum_{i=1}^{K} E_i. \quad (11)$$

Previous works have reported encouraging results for the identification of biological dynamics with this descriptor (Passoni *et al* 2005, Braga *et al* 2007, Nobre *et al* 2009).

2.3. Pseudo colouring by self-organizing maps

The SOM proposed by Kohonen is a popular unsupervised neural network model (Kohonen 2001). The SOM quantizes the data space of training data and simultaneously performs a topology-preserving projection of the data space onto a regular neuron (or cell) grid. The SOM structure is usually a regular two-dimensional grid of neurons, though they can be arranged in one-dimensional (line) or three-dimensional (space). Considering D-dimensional input data, each neuron is connected to the inputs by D weights. From another point of view, these weights can be seen as cells built up with vectors of D dimensions. This set of reference vectors is called the SOM codebook. The map cells are related each other by a neighbourhood function. There are no weights that explicitly interconnect the neurons.

During training, in every step one sample vector from the input dataset is taken and a similarity measure is computed between the input vector and all the codebook vectors. The cell whose weight vector has the greatest similarity with the input sample is selected as the best-matching unit (BMU). The similarity is defined by means of a distance measure, typically Euclidean distance.

After finding the BMU, the codebook is updated. The reference vectors of the BMU and its topological neighbours (according to the neighbourhood function) are changed in order to be 'closer' to the input vector in the input space. This adaptation procedure stretches the BMU and its topological neighbours towards the sample vector. The adaptation is given by:

$$W_j(n+1) \leftarrow W_j(n) + \eta(n)h_{ji}(n)[X(n) - W_j(n)], \quad (12)$$

where n is the iteration number, j is the neuron index that is considered in the current iteration, W_j is the prototype vector of cell j, $\eta(n)$ is the learning rate, $h_{ji}(n)$ is the neighbourhood function defined centred on the BMU, and $X(n)$ is the input data vector presented. Usually, both learning rate and the

neighbourhood function radius decrease as iterations progress.

Once trained, there are different options for the SOM to be visualized and analysed. A matrix called the unified distance matrix (U-matrix) contains distances between the codebook vector of each cell and those of their neighbours, and its graphical representation is widely used (Vesanto 1999, Vesanto and Sulkava 2002, Vesanto *et al* 2003). Data samples can be projected onto the SOM by means of their BMU. Similar data will be projected in near cells.

In order to evaluate the quality of the map, two types of errors are considered: the quantization error and topographic error (Vesanto and Sulkava 2002, Vesanto *et al* 2003). They tend to minimize when the map vectors perform an organized projection of the training pattern according to a similarity criterion. The quantization error is computed as:

$$E_{\mathrm{Q}} = \frac{1}{N}\sum_{i=1}^{N}\|x_i - m_i\|, \tag{13}$$

where x_i, $i = 1, 2..., N$ are the training data, m_i is the BMU corresponding to datum x_i, and N is the number of data.

The topographic error is helpful in assessing whether the data topology was preserved after training. It considers the BMU and the second BMU, defined as the cell whose prototype vector is the second nearest from an input data. This error is computed as:

$$E_{\mathrm{T}} = \frac{1}{N}\sum_{i=1}^{N}u(x_i), \tag{14}$$

where $u(x_i) = 1$ if the BMU for datum x_i is not equal to the second BMU and $u(x_i) = 0$ if it is equal.

Once the map is properly trained, colours can be heuristically assigned to cells according to the distance between prototype vectors. The colour coding is such that topological nearby cells will have similar colours and those far away according to this criterion will have distinct colours. Using this coloured map, a colour can be assigned to each input data according their BMUs (Passoni *et al* 2013b).

To assign colours, we followed the next steps.

- The codebook matrix is projected into a two-dimensional space by principal components analysis (PCA).
- The PCA codebook coordinates are scaled in the [0, 1] range.
- Colours are assigned to each cell of the PCA codebook coordinates using an RGB palette, selected to give a well differenced picture on most LCD monitors.

2.4. Processing pipeline

The next sections correspond to the steps of the method we propose.

2.4.1. Step 1: image acquisition. Given the optical setup, acquire a sequence of images. Each pixel is represented by a temporal series.

2.4.2. Step 2: feature extraction. Compute descriptors presented in section 2.2 for each pixel of the image stack, arranging them in vectors. A dataset including one vector for each pixel is obtained.

2.4.3. Step 3: feature selection. Select a heuristic subset of descriptors

2.4.4. Step 4: SOM training. Feed the SOM with a vector assembled with the descriptors selected.

The SOM dimensions (the number of cells and their arrangement) are chosen from a growing algorithm that weights the quantification and topographic errors. Training is stopped when these quality parameters achieve stationary behaviour.

The SOM is initialized as a 2D hexagonal grid with a Gaussian neighbourhood. Training patterns are normalized to the [0, 1] range and the initialization is done using lineal mapping of the training data. The SOM toolkit for Matlab®, from the Laboratory of Computer and Information Science (CIS) at the Helsinki University of Technology, is used.

2.4.5. Step 5: SOM visualization. Visualize the trained SOM choosing a proper colouring code for the codebook as explained in section 2.3, so pixels with similar temporal behaviours will be coloured with similar colours and, conversely, pixels with different temporal behaviours will be coloured with different colours. Identify the areas of the map according activity of the temporal series.

2.4.6. Step 6: pseudo coloured image creation. Create a new colour image, assigning the colour of each pixel, taking the colour of the SOM cell that is the BMU for the vector of the pixel. To improve automatic detection, different processes could be carried out, like changing the colour model, or filtering a particular colour plane.

2.4.7. Step 7: performance evaluation. Evaluate whether the image clearly shows the region of interest according to an expert opinion. If so, the model is accepted; otherwise return to step 3.

The processing pipeline is represented in figure 3.

3. Experiments

In this section, experiments for applying the algorithm proposed are given. Each one has its correlated sections, showing results in the subsequent section 4.

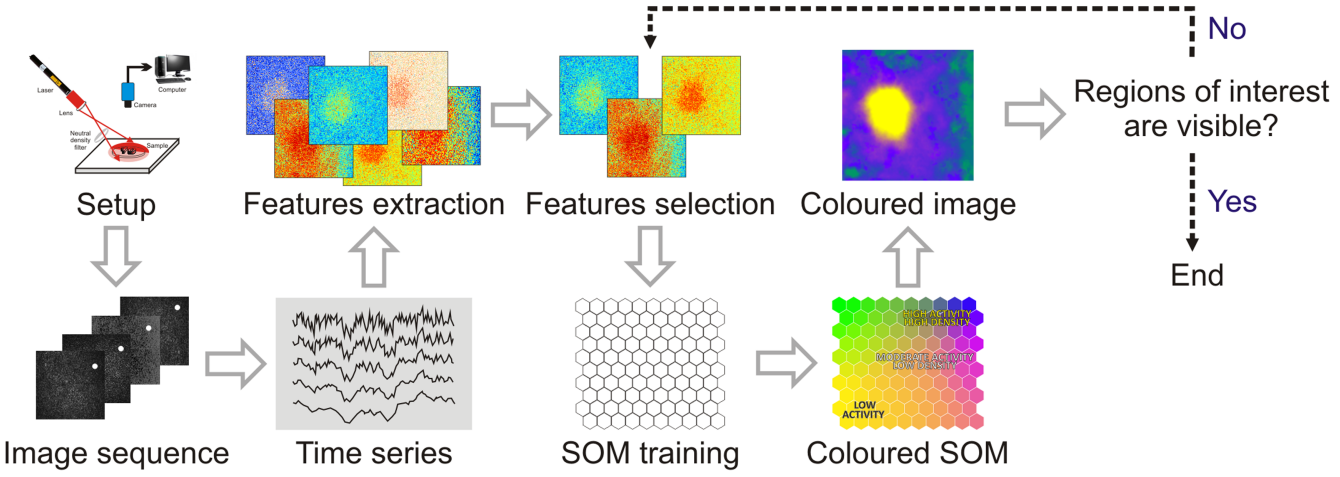

Figure 3. Proposed processing pipeline.

3.1. Activity test in a simplified situation using a paint drying experiment

For this experiment we built a stack of synthetic images using 400 experimental frames obtained with uniformly painted surfaces in different drying stages.

The background of these images (300 × 300 pixels) was taken from one of the stages (180 min drying time) and the centre was replaced by a square region taken from a different stage (210 min drying time, 100 × 100 pixels). Therefore, this image stack showed the activities corresponding to two different known drying states.

In order to train the SOM, these synthetic images were pre-processed using time-domain descriptors. They were preferred because of their low computational cost (Sendra *et al* 2010). It is important to note that these descriptors by themselves did not provide a compound image with an acceptable difference between the two drying regions. We considered an intensity time series from two types of areas: the central area and the border area, using feature vectors with three components corresponding to the time-domain descriptors: SCC, WGD, and AD.

The SOM was trained using an array of 25 by 25 cells.

3.2. Inhomogeneous illuminated surface of a wet painted sample

For this experiment, we tested a coin covered with paint during its drying process. It was expected that the bas-relief of the coin details, being covered by a thin layer of paint, would dry faster than the remaining deeper regions. So, this different speckle activity could be used for revealing the hidden topography.

A neutral density filter ($D = 0.5$) was introduced in the experimental setup in order to cover half of the illuminated region. In this way, both parts, undergoing the same dynamic process, should lead to similar measurements but under different illumination. The process should be robust against inhomogeneous illumination. There was some inhomogeneity in the illumination due to the use of spherical wave, but it was small in comparison with that introduced by the filter. No topographic details of the coin could be perceived in the speckle images before processing (see figure 4). We propose this experiment to find a process able to identify automatically the regions according to their degree of 'activity' (more or less wet depending on the thickness of the paint layer) regardless of the inhomogeneity of illumination.

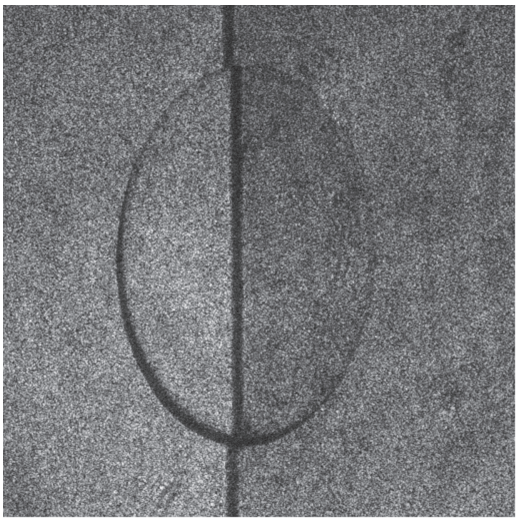

Figure 4. Illumination inhomogeneity. A speckle image before processing.

In this case the SOM is successfully trained with three features vectors, the time-domain descriptors: SCC, SA and FG.

3.3. Bruising detection in apples

Impact damage is one of the quality defects that is most likely to be found in fruits. It has been addressed using a single descriptor at a time (Pajuelo *et al* 2003, Zdunek *et al* 2007, Romero *et al* 2009). This paper proposes the use of a set of descriptors and a SOM for improving automatic recognition of regions of interests such as bruises.

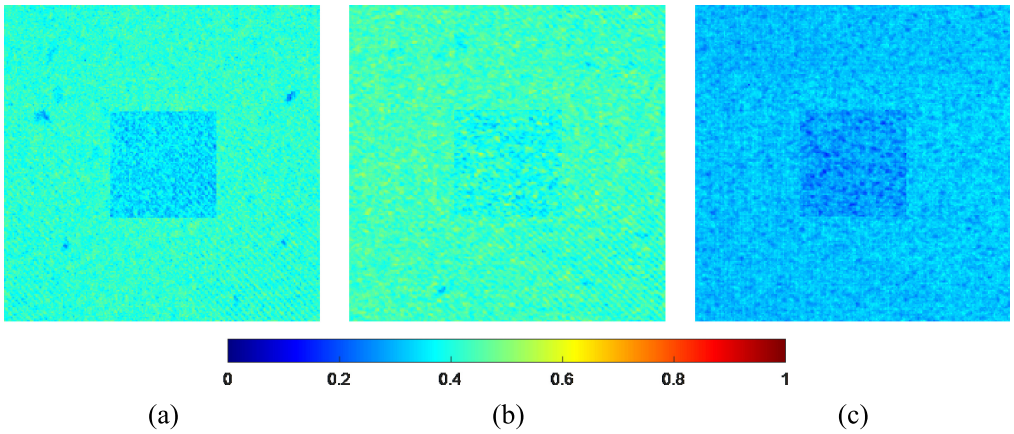

Figure 5. Descriptor images for the painting time experiment. (a) SCC, (b) WGD ($p = 5$) and (c) AD.

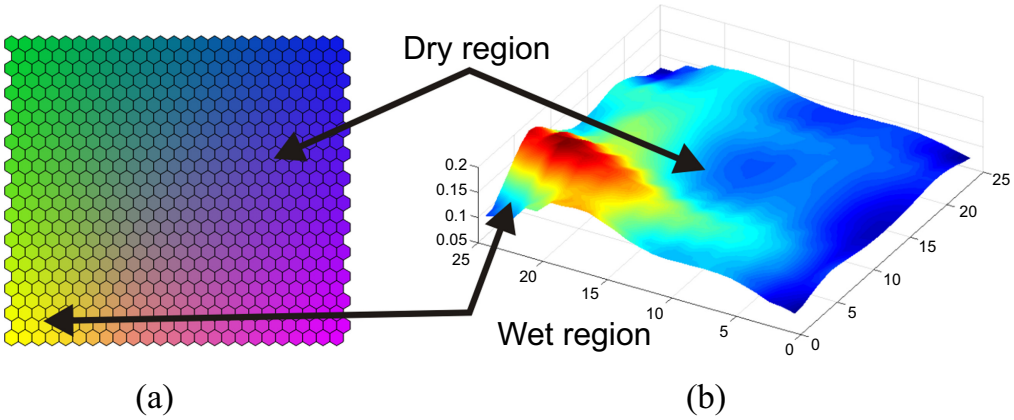

Figure 6. SOM obtained for simulation experiment. (a) SOM coloured by similarity. (b) Distance matrix, where higher levels (red) separate areas of high distance codebooks.

An experiment was carried out hitting apples without any previous damage, red delicious type, with a steel sphere (diameter = 21.9 mm and weight = 133.6 g) from 20 cm height. The bruising produced could not be detected by visual inspection.

Several images in short sequences (less than 100 images), similar to those shown in figure 2, were acquired immediately after the hit in the same experimental conditions. Three descriptors were selected for the SOM to be successfully trained: DR, SA and SWE.

The growing algorithm generated a 25 × 25 cells map. The SOM was trained considering two types of areas: healthy apple tissue and bruised.

Considering the results of other experiments, new pseudo coloured images were created using the previously trained SOM.

4. Results

In this section, results obtained from all the experiments are presented and discussed. Images showing features used in each case and results obtained by SOM processing are given.

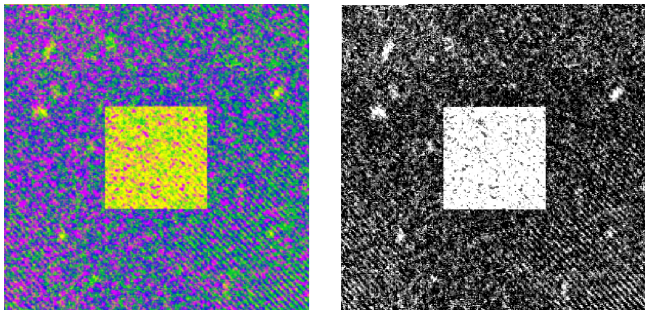

Figure 7. (a) Sample image coloured with the impact of the BMU using the map shown in figure 6(a). (b) Intensity of the red plane of figure 7(a).

4.1. Activity test in a simplified situation using a paint drying experiment

Images built with values of each descriptor are shown in figure 5. Automatic segmentation of both areas cannot be achieved considering each descriptor individually.

Figure 6 shows the results in different SOM visualization. In the U-matrix (figure 6(b)), a well discriminated region at the bottom left-hand corner is shown. In figure 6(b),

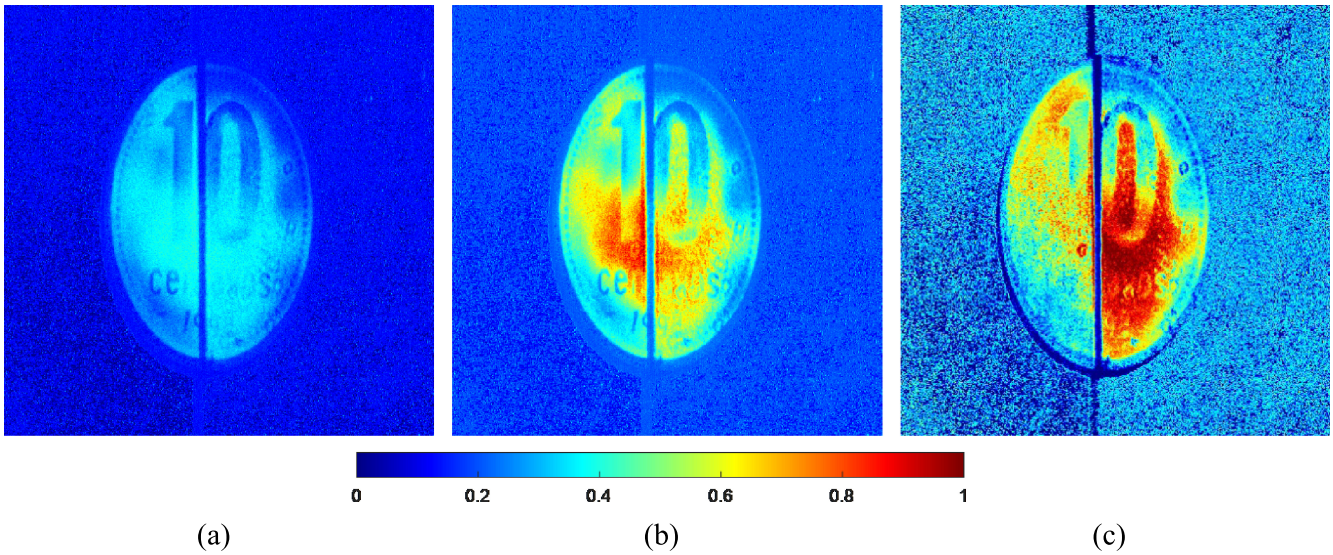

Figure 8. Descriptor images for the inhomogeneous illuminated surface. (a) SCC, (b) SA of consecutive pixel intensities and (c) FG.

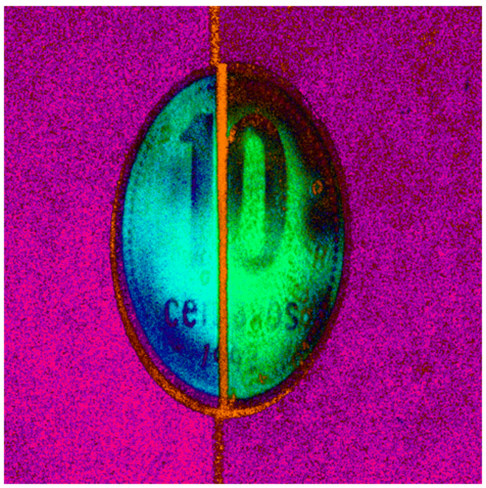

Figure 9. Result from an inhomogeneous illuminated painted coin after pseudo colouring by SOM similarity colouring.

similarity colouring of the map codebook allows easy discrimination of different drying times. Both analyses can be performed in one or other visualization.

The feature vectors of the intensity series belonging to each pixel of the painted sample are fed to the trained SOM. The computed BMU is used to generate an image with the colour of the associated cell (figure 7(a)). To enhance the differences between both analysed regions, the intensity of one colour plane (red) is shown in figure 7(b).

4.2. Inhomogeneous illuminated surface of a wet painted sample

The corresponding features images of the inhomogeneous illuminated painted coin are shown in figure 8.

After training the SOM and building the coloured image according to the BMU impact, figure 9 is obtained. In figure 10(a), the green plane of figure 9 can be observed as an intensity image. In this particular case the green plane enables the best threshold generation for discriminating the painted regions and their relative depth variation. Figure 10(b) shows the intensity profile of a single row, where the background is the darkest, meanwhile the differences between coin regions with variable thickness of coating are clearly visible.

Notice that the word ‘centavos’, the spheres in the rim and the year (1992) can be read in the processed image (figure 10(a)). These details were not perceivable in each descriptor separately (figure 8).

In figure 10, the results are similar in both illumination conditions (left and right halves), while in the FG method, figure 8(c), they are not. In addition, in the descriptors in figures 8(b) and (c) the upper part of the number ‘10’ is contrast reversed with respect to the lower part. In figure 10, the number is mostly evenly darker than its background, i.e. the combination of the three descriptors results is more insensitive to illumination changes.

4.3. Bruising detection in apples

Images from the values of each descriptor are shown in figure 11. It must be observed that the bruised area cannot be automatically segmented in each descriptor image, since its borders are not clearly shown.

After training the SOM, the errors obtained were 0.035 for the quantification error and 0.076 for the topographic error. The U-matrix obtained is shown in figure 12 (left), where two clusters can be discovered corresponding to a bruised area and healthy tissue. Both clusters show low distance values (blue tones), well separated by a high-distance value region (yellow and red tones). By using previous knowledge about this experiment, we identified the clusters as belonging to the different regions. We can conclude that the chosen descriptors are adequate to ‘discover’ the existence of the bruising.

We also obtained another visualization of the internal state of the SOM in order to find new conclusions. A new

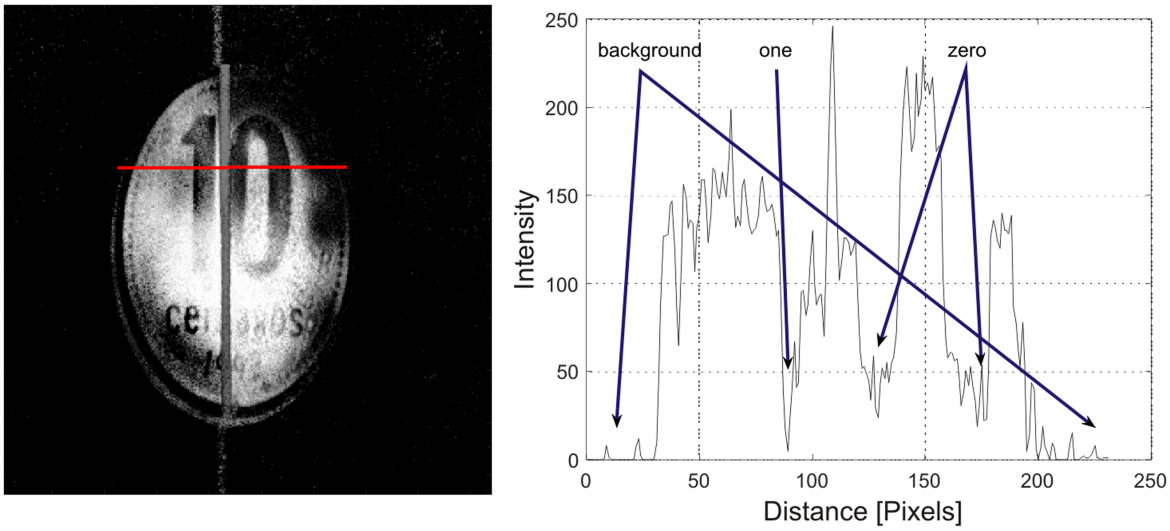

Figure 10. (a) Intensity of the green plane of figure 9. (b) Intensity of the green plane along the red line indicated in (a).

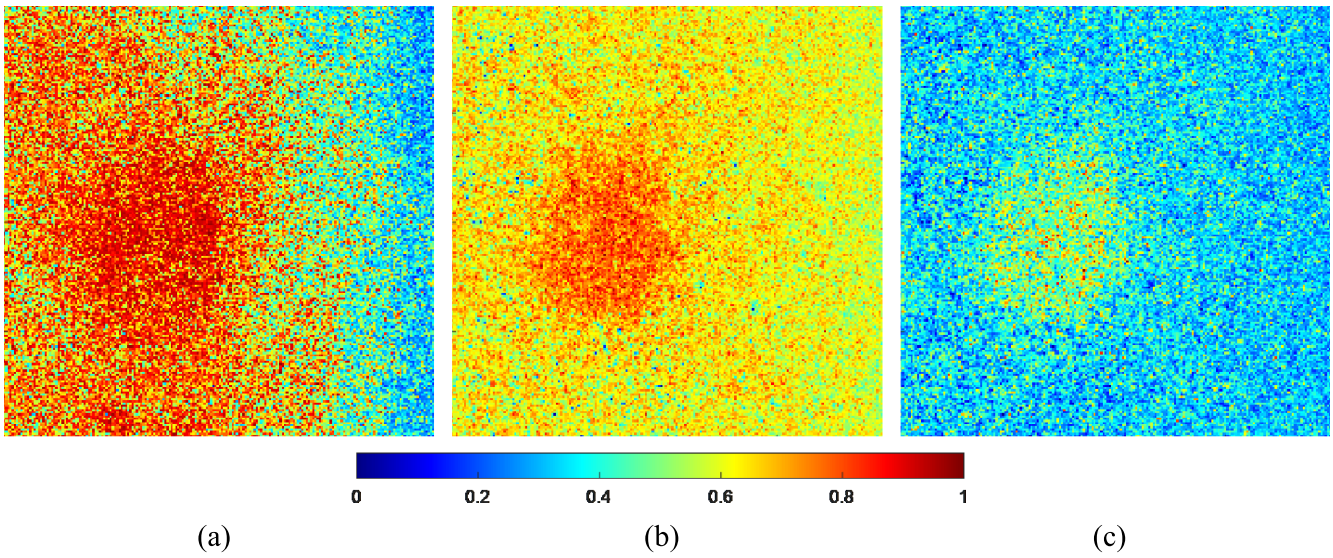

Figure 11. Descriptor images for bruising detection in apples. (a) DR, (b) SA of consecutive pixel intensities and (c) SWE.

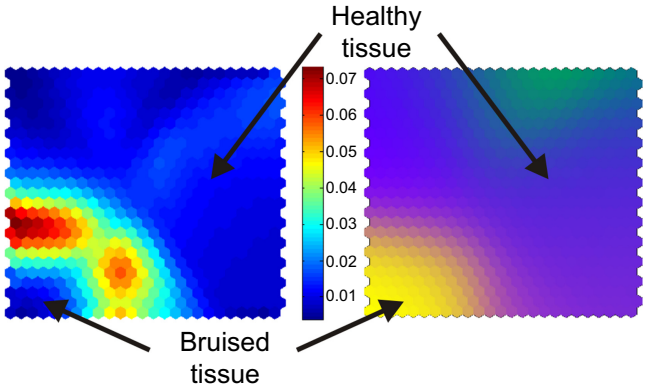

Figure 12. U-matrix (left) and cell prototype vectors after colouring by similarity (right).

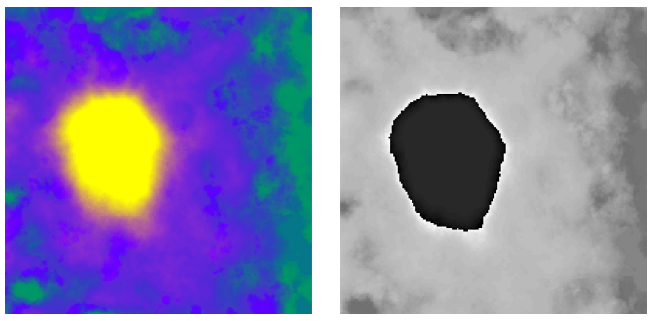

Figure 13. (a) Training sample showing the bruised region in yellow. (b) H plane clearly showing the bruised region in black.

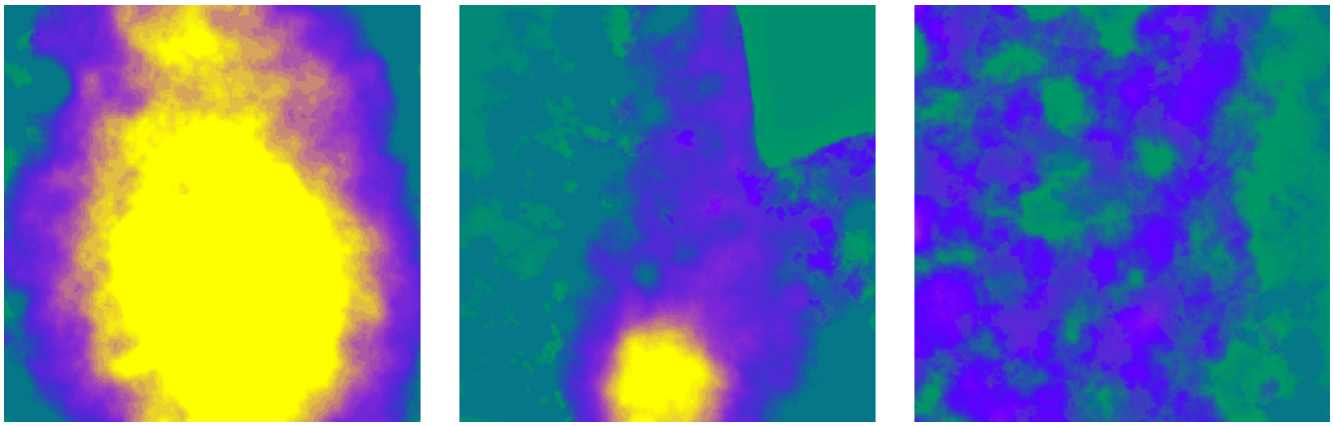

Figure 14. SOM evaluations of test samples for bruising detection in apples. (a) and (b) correspond to two different bruised apples. (c) is the result from a non-bruised apple. The bruised area is shown in bright yellow.

coloured map is obtained, where cells are coloured according to their similarity (cell prototype vectors coloured by similarity, CCS), that can be observed in figure 12 (right). This representation confirms the conclusions obtained from the U-matrix: the 'bruised region' in the bottom left corner (yellow hues) is in agreement with the bruised region in the U-matrix. The violet-green area points correspond to healthy tissue.

As in the other experiments, by taking the BMU for each pixel, a pseudo coloured image was obtained, which is shown in figure 13(a). When computing BMU cells from the training sample, an image is mapped with the CCS colour where each BMU impacts.

To improve the automatic detection, a colour map change is carried out (from RGB to HSV colour model). Then the H plane is filtered to provide a sharp definition of the bruised area. The H plane of the HSV colour model of the latter is shown in figure 13(b). The well-defined black bruise is easily detected and therefore a quantitative assessment of this area can be easily performed.

The trained SOM was recalled with a test set of speckle sequences that were measured under the same protocol, obtaining the results shown in figure 14, where the existence of yellow regions discovers bruising in different samples, if they exist. In figures 14(a) and (b), a case with an enhanced bruise region is presented and in figure 14(c), a case with no bruise region is shown. The latter case is the result of a speckle sequence acquired without bruising.

5. Discussion

It can be seen from the results that the combination of descriptors may provide better results than the use of only one. Details that cannot be distinguished using only one appear in the SOM processed image in a perceivable way. The bruised region in the apple is clearly distinguished so that pixels can be counted and its frontier established (or drawn). The processed image is more robust to illumination changes than the separate descriptors.

The most adequate descriptors have to be chosen for each application as not any combination would provide the best results.

If needed, more descriptors could be included as only the training procedure is computer intensive. The pseudo coloured image creation procedure for new unknown samples requires substantially less computer time.

The fact that the procedure is driven by the phenomenon itself is an advantage with respect to supervised methods in that it is able to discover unknown activity similarities.

6. Conclusion

In this work we proposed the use of SOMs for segmentation of regions of similar activity in dynamic speckle images. The procedure is driven by the sample dynamics and it does not require supervision. A SOM is trained using a set of descriptors and the result is used to identify unknown samples. Its scope is not restricted to the analysed cases but it includes many other possible applications.

We exemplified it by using experiments to identify diverse regions such as paint drying state and its underlying surface details and in biological specimens such as the bruising in apples segmentation.

The methodology proposed is based on an optical acquisition setup together with a multi descriptor approach to characterize dynamic speckle images.

We tested the procedure on a very simple situation: a set of activity images was built with two regions of speckle due to paint in different drying states. It was successfully segmented using the SOM processing while the participant descriptors did not individually perform so well.

We also tested the procedure using a sample consisting in a coin covered with paint where no topographic detail could be perceived. The details were recovered using the SOM procedure. The robustness of the activity similarity

segmentation was simultaneously verified by using two regions with similar activities and different illuminations. These results were encouraging.

The methodology proposed also allowed the detection of bruised regions in apples when they were not yet visible. The SOM trained with descriptors from a video sequence permitted the discovery of bruises in samples from other experiments. The process improves the results obtained with single descriptors, as in most of the previously published works. This is particularly true even when the registered sequences are not very long, that is, less than 100 images, which involves a short acquisition time. The result could allow the automatic measuring of the bruised area as well as the determination of its perimeter.

It must be considered that although in practice the model must be previously trained according to the experiment particularities, its recall demands low computational cost. This characteristic would allow its inclusion into an on-line process for recognition of regions of interest in an artificial vision system.

Acknowledgments

This work was supported by CCT La Plata Consejo Nacional de Investigaciones Científicas y Técnicas (CONICET), Comisión de Investigaciones Científicas de la Provincia de Buenos Aires, by Facultad de Ingenieria, La Plata National University, by Facultad de Ingeniería, Mar del Plata National University and by PICT 2008-1430, Grant by Agencia Nacional de Promoción Científica y Tecnológica, Argentina.

References

Arizaga R, Cap N L, Rabal H and Trivi M 2002 Display of local activity using dynamical speckle patterns *Opt. Eng., Bellingham* **41** 287–94

Braga R A Jr, Horgan G W, Enes A M, Miron D, Rabelo G F and Barreto Filho J B 2007 Biological feature isolation by wavelets in biospeckle laser images *Comput. Electron. Agric.* **58** 123–32

Dai Pra A L, Passoni L I, Sendra G H, Trivi M and Rabal H J 2015 Signal feature extraction using granular computing. Comparative analysis with frequency and time descriptors applied to dynamic laser speckle patterns *Int. J. Comput. Intell. Syst.* **8** (sup2) 28–40

Engelbrecht A P 2007 *Computational Intelligence: an Introduction* 2nd edn (Chichester: Wiley)

Etchepareborda P, Federico A and Kaufmann G H 2010 Sensitivity evaluation of dynamic speckle activity measurements using clustering methods *Appl. Opt.* **49** 3753–61

Fujii H, Asakura T, Nohira K, Shintomi Y and Ohura T 1985 Blood flow observed by time-varying laser speckle *Opt. Lett.* **10** 104–6

Guyon I and Elisseeff A 2003 An introduction to variable and feature selection *J. Machine Learning Res.* **3** 1157–82

Guzmán M, Meschino G J, Dai Pra A L, Trivi M, Passoni L I and Rabal H 2010 Dynamic laser speckle: decision models with computational intelligence techniques *Proc. SPIE* **7387** 738717

Kohonen T 2001 *Self-Organizing Maps (Springer Series in Information Sciences)* (Berlin: Springer-Verlag)

Meschino G, Murialdo S, Passoni L, Rabal H and Trivi M 2010 Biospeckle image stack process based on artificial neural networks *Conf. Proc. IEEE Eng. Med. Biol. Soc.* **2010** 4056–9

Nobre C M B, Braga R A Jr, Costa A G, Cardoso R R, da Silva W S and Sáfadi T 2009 Biospeckle laser spectral analysis under inertia moment, entropy and cross-spectrum methods *Opt. Commun.* **282** 2236–42

Pajuelo M, Baldwin G, Rabal H, Cap N, Arizaga R and Trivi M 2003 Bio-speckle assessment of bruising in fruits *Opt. Lasers Eng.* **40** 13–24

Passoni I, Dai Pra A, Rabal H, Trivi M and Arizaga R 2005 Dynamic speckle processing using wavelets based entropy *Opt. Commun.* **246** 219–28

Passoni I, Rabal H, Meschino G and Trivi M 2013a Probability mapping images in dynamic speckle classification *Appl. Opt.* **52** 726–33

Passoni L I, Dai Pra A L, Scandurra A G, Meschino G J, Weber C, Guzmán M, Rabal H and Trivi M 2013b Improvements in the visualization of segmented areas of patterns of dynamic laser speckle *Advances in Self-Organizing Maps Advances in Intelligent Systems and Computing* ed P Estévez *et al* (Heidelberg: Springer) pp 163–71

Rabal H J and Braga R A (ed) 2008 *Dynamic Laser Speckle and Applications* (Boca Raton, FL: CRC Press)

Romero G G, Martinez C C, Alanís E E, Salazar G A, Broglia V G and Álvarez L 2009 Bio-speckle activity applied to the assessment of tomato fruit ripening *Biosyst, Eng,* **103** 116–9

Rosso O A, Blanco S, Yordanova J, Kolev V, Figliola A, Schürmann M and Başar E 2001 Wavelet entropy: a new tool for analysis of short duration brain electrical signals *J. Neurosci. Methods* **105** 65–75

Sendra G H, Dai Pra A L, Passoni L I, Arizaga R, Rabal H J and Trivi M 2010 Biospeckle descriptors: a performance comparison ed A Albertazzi Goncalves Jr and G H Kaufmann *Proc. SPIE* **7387** 73871K

Vesanto J 1999 SOM-based data visualization methods *Intell. Data Analysis* **3** 111–26

Vesanto J and Sulkava M 2002 Distance matrix based clustering of the self-organizing map *Proc. Artificial Neural Networks—ICANN 2002: Int. Conf. (Madrid, Spain, 28–30 August 2002)* ed J R Dorronsoro (Berlin: Springer) pp 951–6

Vesanto J, Sulkava M and Hollmen J 2003 On the decomposition of the self-organizing map distortion measure *Proc. Workshop on Self-Organizing Maps (Hibikino, Kitakyushu, Japan)* pp 11–6

Zdunek A, Muravsky L I, Frankevych L and Konstankiewicz K 2007 New nondestructive method based on spatial-temporal speckle correlation technique for evaluation of apples quality during shelf-life *Int. Agrophys.* **21** 305–10